Journal of Engineering and Technological Advances (JETA)
https://jeta.segi.edu.my/index.php/segi
2023 Vol. 8 No. 1

SIMULATION OF STRESS ANALYSIS FOR MULTIPLE TRUSS STRUCTURES FOR DUAL SEATED ROLL CAGE CHASSIS

[1]Badrulhisam, N.H.*, [2]Sajib, S.A., [1]Teo, H.H., [3]Ahmad Zamri, A.A.

[1] Centre for Advances Engineering Design, Faculty of Engineering, Built Environment and Information Technology, SEGi University, 47810 Petaling Jaya, Selangor, Malaysia.
[2] Faculty of Engineering, Built Environment and Information Technology, SEGi University, 47810 Petaling Jaya, Selangor, Malaysia.
[3] Faculty of Engineering, Built Environment and Information Technology, MAHSA University, 42610 Jenjarom, Selangor, Malaysia.

* Corresponding Author: najmihaziq@segi.edu.my   TEL: (+603)- 61451777

Abstract: In recent years, automotive chassis has developed tremendously. This includes the roll cage chassis type which has a higher centre of gravity. This will require an optimum number of truss members to ensure the rigidity and safety of the chassis and user. This research paper aims to analyse the roll cage chassis frame using static analysis simulation by removing truss members at the bottom of the chassis for each design. Carbon steel was employed for all chassis designs. Then, static analysis simulation was done using Autodesk Inventor 2023. From the static analysis, a load equal to 6300 N was applied to the chassis. The safety factor, von Misses stress, 1st principal stress, and 3rd principal stress were analysed and compared for each of the designs. The result shows that the lowest safety factor starting from Design 1, Design 2 and Design 3 with the values of 2.13, 1.85, and 3.24, respectively. For the 1st principal stress, the values are 97.39 MPa, 329.5 MPa, and 104 MPa for Design 1, Design 2, and Design 3, respectively. This result is good as the ultimate strength of carbon steel is 695 MPa. While for the 3rd principal stress, the values are 20.2 MPa, 96.4 MPa to 37.6 MPa for Design 1, Design 2, and Design 3, respectively. In conclusion, removing a few truss members will affect the static analysis performance. It is determined that Design 2 has an optimum truss members number compared to the other two designs.

Keywords: Safety factor; Von Misses stress; 1st principal stress; 3rd principal stress; Multiple truss structure

1. Introduction

Transportation by car has become a necessary in our everyday lives, with no middle- or upper-class household with a steady income can function without at least one vehicle. It saves both time and effort to get to a destination. In terms of design, modern rise buggies have come a long way from the original Meyers-Manx adaptations, which consisted mostly of fibreglass bodywork with roll bars and large windshields mounted on top of Volkswagen Insect chassis to create super-fun dune buggy clones (Abbas & Mohammed, 2015). This advancement is also supported by various new design approaches such as Generative Design in the technical fields (Buonamici et al., 2020). Since they were rear-wheel drive and had amazing sand footing, ancient Creepy crawlies made the most sense possible. Furthermore, they were inexpensive and easy to customize. Nowadays, the hill buggy has advanced into so much more. Cutting-edge forms are moreover known as side-by-side all-terrain vehicles and they are as much for hard-charging and obligations as they are simple hill cruising.

The application of a roll cage to a vehicle is really intriguing. When individuals first began modifying these automobiles, they used to remove some of the most important components of the vehicle, which would result in a new issue (Garg & Raman, 2013). The vehicle was unable to support its own weight and was thus deemed weak by the authorities. In most cases, the addition of a roll cage to a vehicle would boost the vehicle's overall strength. Because these cars were prone to rollovers and other major accidents, the passengers and drivers would be better protected in the event of a disaster. As a result, roll cages are now being used in National Association for Stock Car Auto Racing (NASCAR) competitions, which provides superior safety for drivers and passengers since this racing competition is always very prone to collisions (Reiter et al., 2017; Safiuddeen et al., 2021).

It is a frame that has been meticulously designed and produced to be installed within (or surrounding, in which case it is referred to as an Exo cage) a vehicle's passenger compartment in order to prevent passengers from being injured. In the past, roll bars have also been used on row crop tractors to assist in harvesting. Roll cages are a common feature of modern tractors, and they are often integrated into the car. The original crash test consists of slamming a real car into a human dummy in order to determine the level of physical damage. Because of the changing requirements of the automotive industry, roll cages have grown greatly from what they were at their inception. Investigating new production processes attribute for new materials may be able to alleviate this situation (Safiuddeen et al., 2021; Soundararajan et al., 2021).

The design and development of a roll cage involves a number of steps, including the selection of materials, the design of the structure, the determination of the cross-section, and the use of computational tools. The material selection for the frame is one of the most critical design choices that was made, and it has a significant impact on the overall safety, reliability, and performance of any automobile design. A thorough investigation was carried out, and components from a variety of categories were examined in order to ensure that the best material was selected (Gautam et al., 2020; Mishra, 2017).

The addition of a roll cage increases the overall handling performance of a vehicle as well as its centre of gravity. Roll cages contribute to the overall strength of the chassis, which is advantageous in racing. It is most usual to find racing cages that are bolted or welded into place, with the former being simpler and less costly to install and the latter being more robust. It is a single bar that runs behind the driver and provides some rollover protection in the event of a collision. (Li & Feng, 2020). In general, for the static analysis, simulation can be utilised to study the chassis design integrity in terms of the safety factor, von Misses stress, 1st principal stress, and 3rd principal stress. With the static analysis, chassis strength and structural optimization can shorten the design development and design cycle of vehicular products (Li & Feng, 2020).

To date, there are only few studies that investigate the performance of roll cage bar chassis for buggy application compared to the Go-Kart chassis. In this research paper, the effect of the removal of truss members from a chassis bottom by means of static analysis of three chassis designs was done using Autodesk Inventor 2023. The safety factor, von Misses stress, 1st principal stress, and 3rd principal stress were analysed and the most optimum design was determined.

2. Materials and Methods

The Ariel Atom in **Figure 1** served as an inspiration for the design of the vehicle. There are some parallels between it and a buggy. However, it is fitted with a roll cage. The design is a cross between a Formula One vehicle and a buggy in appearance. The Atom is the vehicle that comes the closest to the design of the buggy used in this study.

Figure 1. Ariel Atom car using multi truss structure chassis (Abbas & Mohammed, 2015)

The whole design and stress analysis of this study was done in Autodesk Inventor 2023. The design was made using 2D and 3D sketches stitched together using the program. The whole sketch was done in millimetres and saved as a part (.ipt) file. Then a new assembly file was created using the inventor and the overall 3D sketch was placed inside the space. The Inventor frame generator was used to produce the frame out of the sketch. The frame size used for this project was ANSI 1 ½ × 0.145, which is the tubular circular type of material. After the sketching of the chassis structure was done, the frame generator function was used to complete the 3D structure of the chassis. Then, the Miter command was used to attach the corners where the pipes meet. The Miter function was used to give the whole design a refined look. The Miter function helps replicate welded parts digitally in Inventor (Dimitrijevic & Dimitrijevic, 2020). After the finishing was done to the designed model, the model was digitally tested in an environment. There are several testing environments present in the Inventor. For this study, the stress analysis test was performed to evaluate if the designed model can take the amount of force required. The stress analysis test basically simulates theoretical loads added to the structure and the deformation of breaking that might happen due to loads applied on the body (Munford & Normand, 2015). The tests were done on a single design with three phases of changes where each test was done on reducing members compared to the previous design used in the test. The test was a simple stress analysis test conducted on three different designs. The designs were generally made with the frame generator feature and using miter and notch tools present in Autodesk Inventor 2023. The whole process of the design was made from a wireframe skeleton which is three different 2D sketches stitched together using several 3D sketches. The sketch was then taken into the frame generator and the ANSI circular pipe 1 ¼ × 0.191 was used to make the design. The material selected for these designs was high carbon steel. After the basic construction of the model was done, there were interferences that needed to be solved in order to make an errorless design. To solve the interferences, two mentioned features were used. The features eliminate sections of each member in a contact zone making a flawless corner or end. Miter was used to solve multiple members automatically using the intelligence of the software. Furthermore, by using the notch feature, each member was solved against one another. **Table 1** and **Figure 2** show the truss members that was removed and the location of the truss members respectively. The load applied to the top of the chassis is 6300 N taking into consideration of the weight for the structure and two passengers of mass of 80kg.

Table 1. Truss members included for the three designs

	Truss Member 1	**Truss Member 2**	**Truss Member 3**
Design 1	✓	✓	✓
Design 2		✓	✓
Design 3			✓

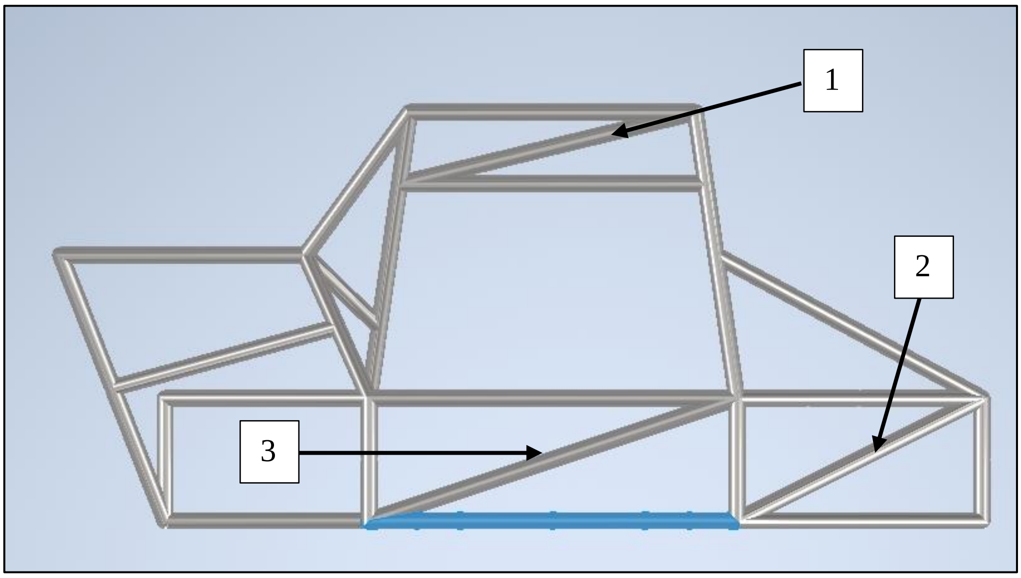

Figure 2. Location of the truss members for the roll cage chassis structure

3. Results and Discussion

3.1. Safety Factor

In **Figure 3(a)**, it can be seen that when a load of 6300 N is applied to the body, the safety factor has a maximum limit of 15 and a minimum limit of 2.13 for Design 1. It can be assumed that a body with a safety factor of more than 1 is preferably safe as it will withstand maximum force without breaking (Lai & Xiao, 2012). There is shear bending due to the applied load but the elasticity of high carbon steel can withhold the applied load. Menacho-Mendoza et al. obtained the similar trends of safety factor and indicated that the chassis structure can withstand the force of applied load multiplied with the safety factor (Menacho-Mendoza et al., 2022). **Figure 3(b)** shows that the degree of safety seems to be uniform distributed throughout the chassis structure. When a load of 6300 N is applied to the body, the safety factor has a maximum limit of 15 and a minimum limit of 1.85. The load that is being applied causes shear bending, yet the elasticity of high carbon steel is sufficient to withstand the force that is being applied. In **Figure 3(c)**, it seems that the level of safety present here is distributed uniformly across the chassis structure. The safety factor has a maximum limit of 15 and a minimum limit of 3.24 when a weight of 6300 N is applied to the body. Even if the stress that is being applied results in shear bending, the elasticity of high carbon steel is adequate to ensure that it will not break under the load that is now being applied. Design 3 has the least members and has the highest minimum safety factor compared to other designs presented.

Similar findings were found by Krishnamoorthi S et al. (Krishnamoorthi et al., 2021). The result shows that Design 3 has the highest value of safety factor at the minimum (**Figure 4**). This value means that the design is capable is holding a maximum of 3.24 times the total force applied to the design. The higher value of the safety factor means that the design is safer to use and the susceptibility to failure becomes less. The variation in the safety factor is due to the distribution of the load at the truss joints.

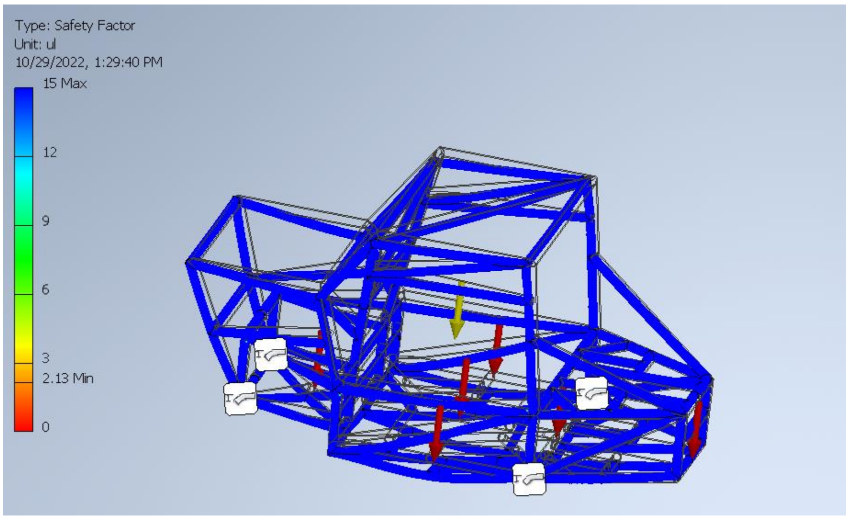

(a)

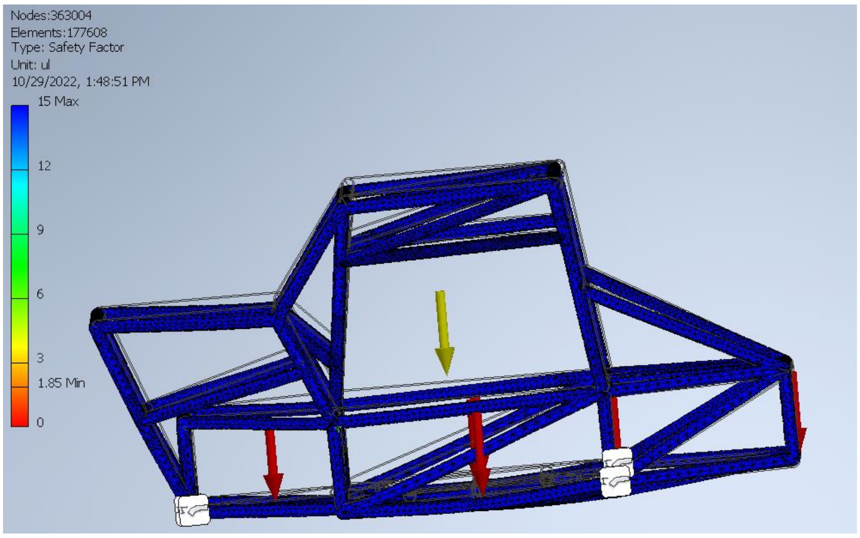

(b)

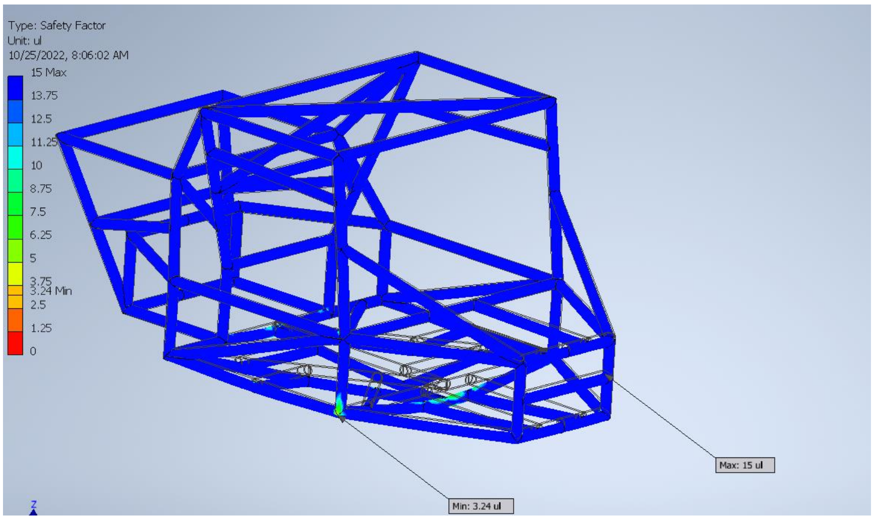

(c)

Figure 3. Comparison of safety factor for (a) Design 1, (b) Design 2, and (c) Design 3

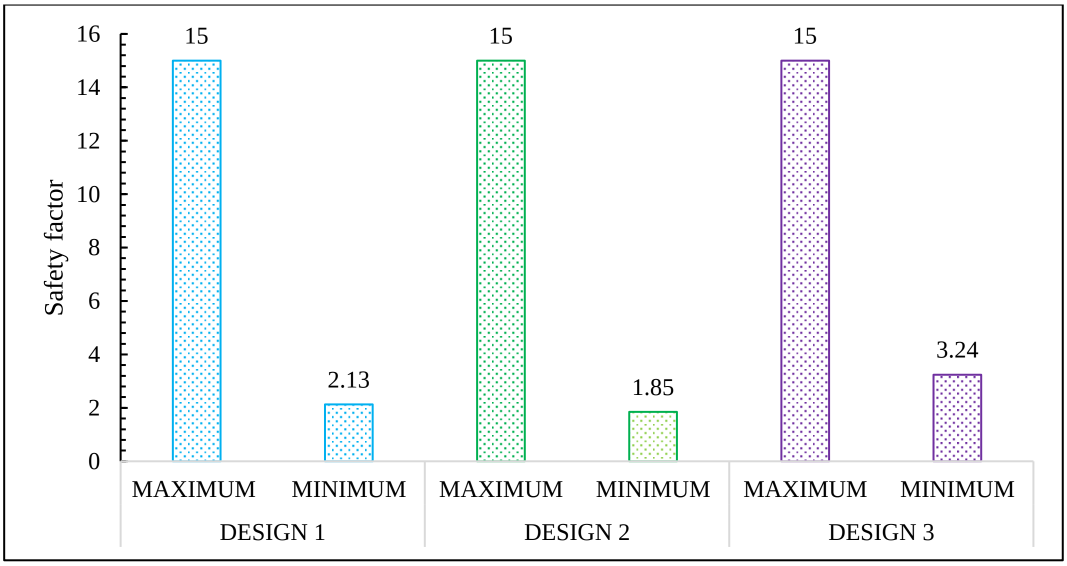

Figure 4. Safety factor variation values for the three designs

3.2. Von Misses Stress

The von Misses stress for Design 1 is at a maximum of 97.35 MPa and minimum of 0 MPa, as shown in **Figure 5(a)**. The maximum stress detected was above each of the constraint positions. The distribution shows that 97.35 MPa pressure on the point above the constraints which is lower than the fatigue value of high carbon steel. The boundary conditions are to be met in this case, as the wheel positions will not be exactly on top of the constraint points and may vary during experimental research of the designed model. The maximum tensile strength of high carbon steel is 685 MPa which is a lot more than the maximum stress induced to the body. In **Figure 5(b)**, there is a maximum von Misses stress of 302.1 MPa and a minimum von Misses stress of -46.9 MPa. The locations of the constraint sites were all above the maximum stress that was measured. The distribution reveals that the point above the restrictions has a pressure of 302.1 MPa, which is less than the fatigue value of high carbon steel. Furthermore, Design 3 in **Figure 5(c)** has a maximum stress of 108 MPa which is lower than the Design 2. This shows that the body is capable of holding the weight more than any other design. The design has higher stress compared to Design 1 which is negligible change but still within the range of high carbon steel tensile strength of 680 MPa. Garg and Raman found that the lower weight-to-strength ratio was the key point for structural superiority. Therefore, removing some of the truss members is not an indicator of the structural strength (Garg & Raman, 2013).

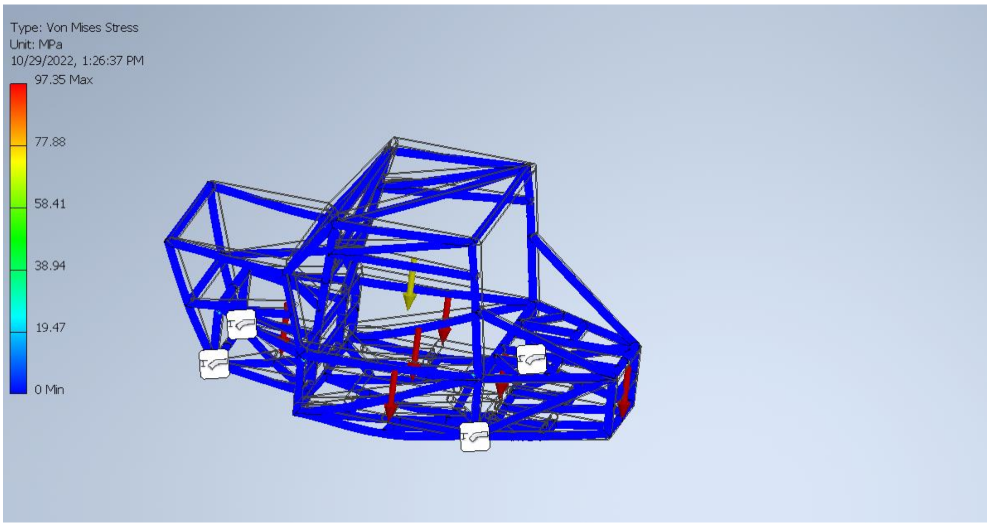

(a)

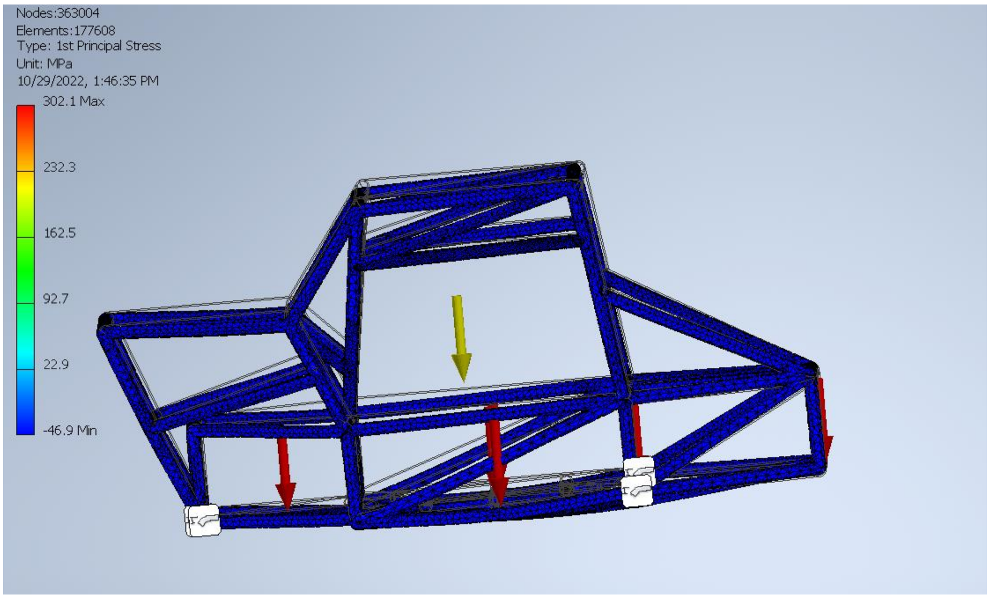

(b)

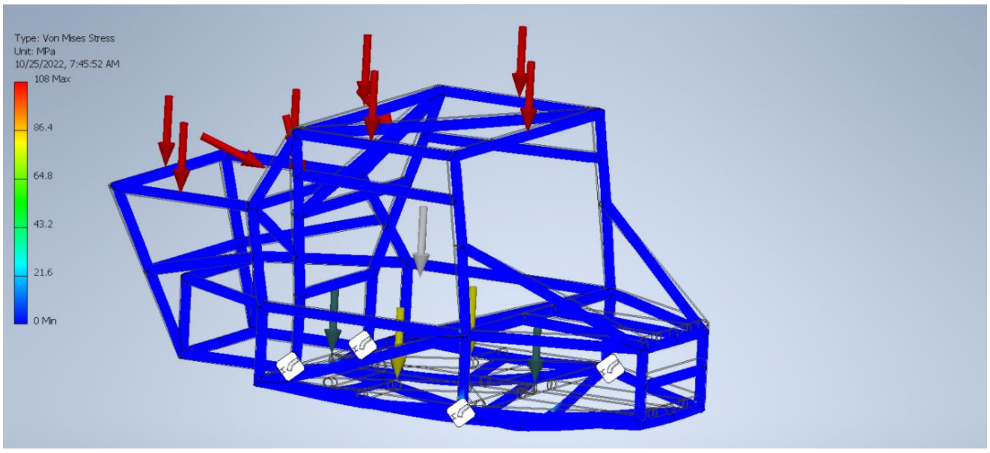

(c)

Figure 5. Von Misses stress variation for (a) Design 1, (b) design 2, and (c) Design 3

The information that is shown in the **Figure 6** demonstrates that there is a variation in the maximum primary stress from design 1 to design 2. The value of the major stress goes from 97.35 MPa to 302.1 MPa after the adjustment. The removal of truss members causes other major truss members to experience an excessive amount of force, which led to the reason of this alteration in the truss structure. However, from Design 2 to Design 3, in which more truss members were removed, this decreases the value of the maximum stress. This was due to the fact that the truss members utilized have an excellent transmission of stress throughout the body (Chauhan et al., 2016).

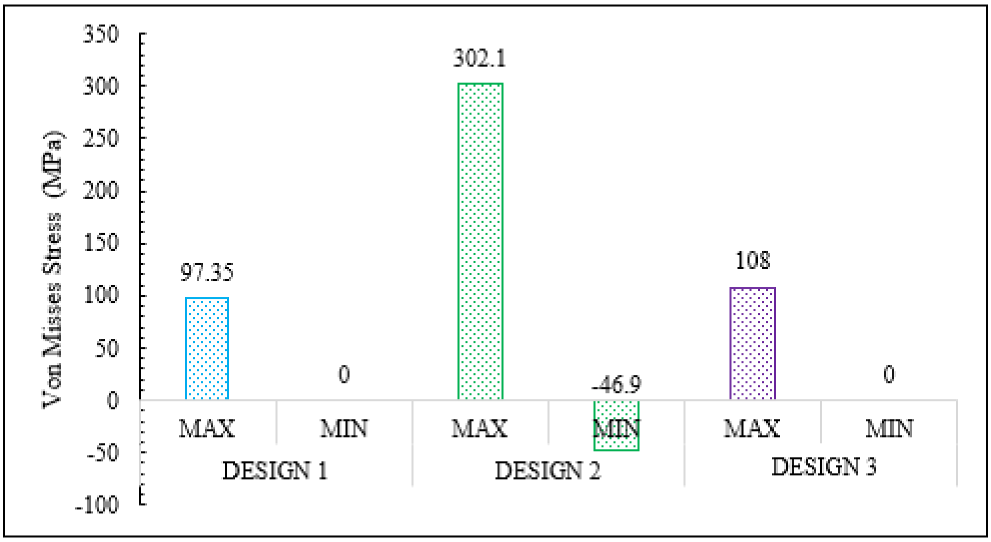

Figure 6. Von Misses stress values variation for the three designs

3.3. 1st Principle Stress

The maximum stress recorded for Design 1 in **Figure 7(a)** is 97.39 MPa and minimum stress is -20.26 MPa. These recorded stresses are normal stress acting towards gravity. The shear force is considered to be 0 MPa. The 1st principal stress is the maximum value of stress in the system. In **Figure 7(b)**, the maximum stress recorded for Design 2 is 329.5 MPa and the minimum stress is -48.1 MPa. On the other hand, the Design 3 in **Figure 7(c)** has a noticeably less stress value compared to Design 2 and slightly more than Design 1. The maximum principal stress recorded for Design 3 is 104 MPa and the minimum stress value recorded is -40.9 MPa. The carbon steel tensile strength is 680 MPa so the body is getting lower stress compared to the maximum allowable stress.

The data presented in the **Figure 8** shows that there is a change in maximum principal stress when the test results is shifted from design 1 to design 2. The principal stress value changes from 97.39 MPa to 329.5 MPa. This was caused due to change in the truss structure, removal of truss members leads to relative higher force in other significant truss members. However, removal of more truss members for Design 3 led to a decrease in maximum 1st principal stress as the truss members used were having a good transfer of stress throughout the body (Prakhar et al., 2017).

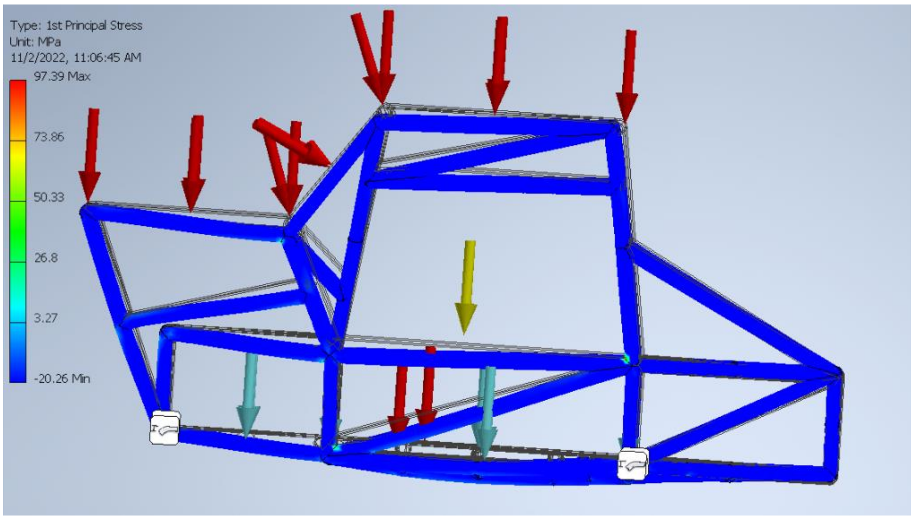

(a)

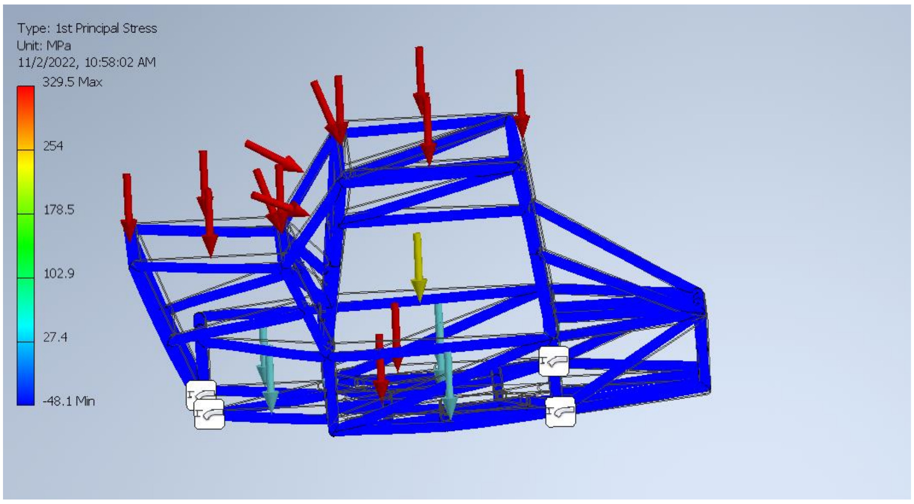

(b)

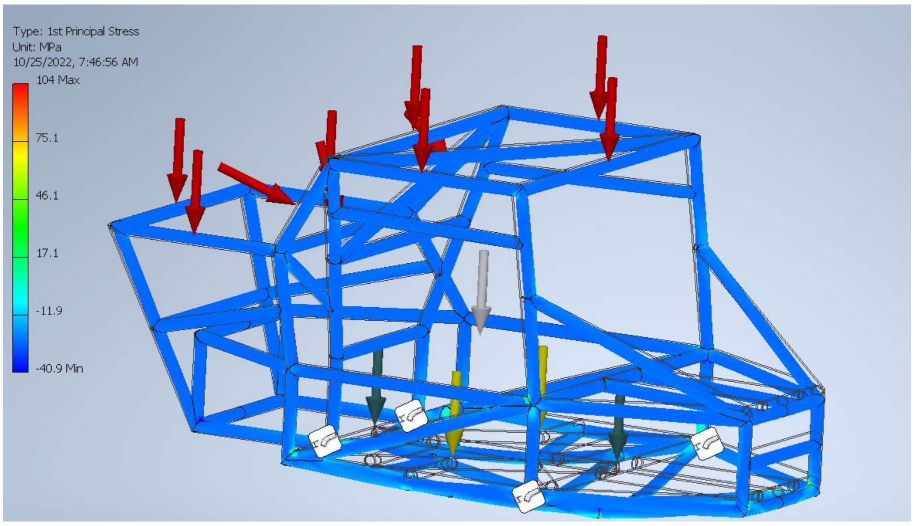

(c)

Figure 7. The 1st principle stress at the joint of the truss members for (a) Design 1, (b) Design 2, and (c) Design 3

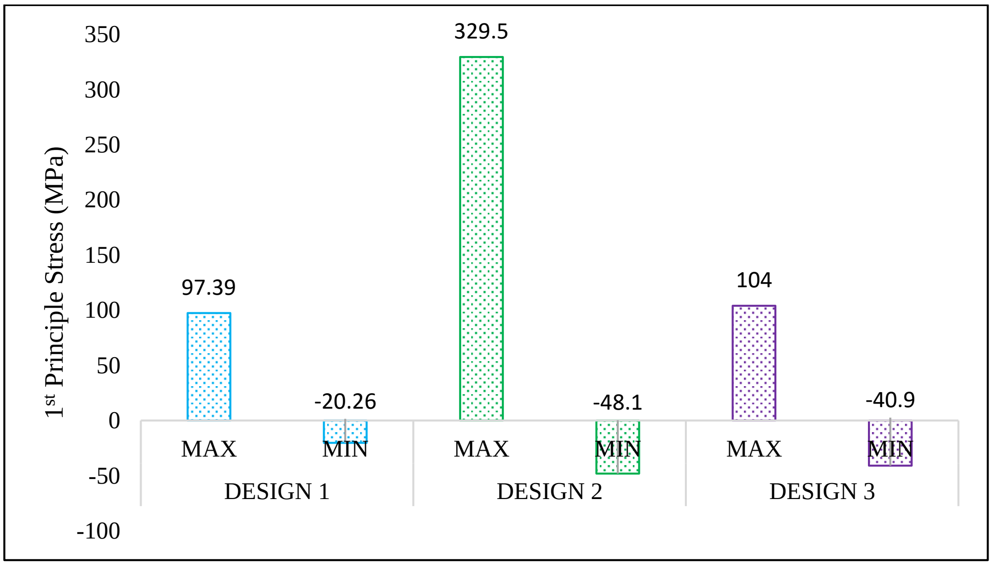

Figure 8. Distribution of 1st principle stress for the three chassis designs

3.4. 3rd Principle Stress

The minimum recorded stress for Design 1 in **Figure 9(a)** is -101.1 MPa and maximum stress recorded was 20.2 MPa. The third principal stress is also known as the normal stress. The data shows that the model is susceptible to high compressive stress at places and has low expansion in most of the places. This can be confirmed by the colour of the stress analysis model. The average 3rd principal stress is between the range of -4 MPa to -25 MPa for the chassis structure.

For Design 2, as shown in **Figure 9(b)**, the minimum recorded stress is -146.9 MPa and the maximum stress recorded was 96.4 MPa. The average 3rd principal stress is between the range of -0.9 MPa to –49.6 MPa for the chassis structure. On the other hand, as shown in **Figure 9(c)**, Design 3 shows the minimum recorded stress is -154.1 MPa and the maximum stress recorded was 37.6 MPa. The average 3rd principal stress is between the range of -0.7 MPa to -39.1 MPa for the chassis structure.

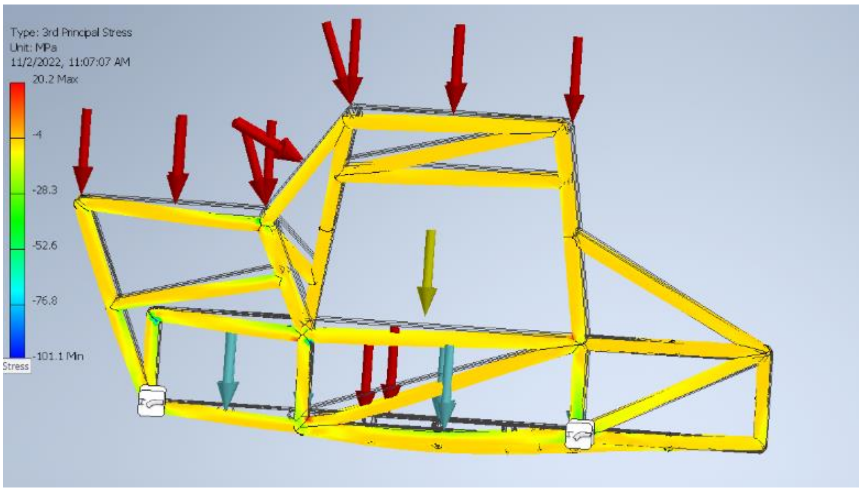

(a)

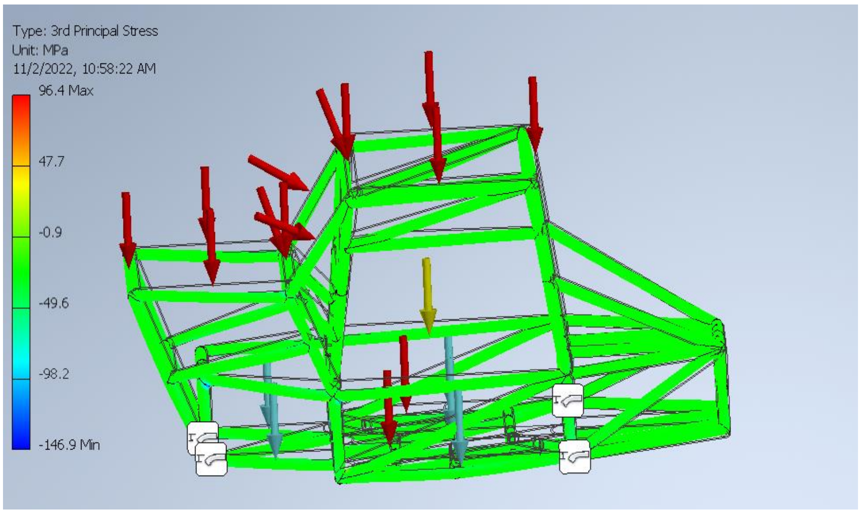

(b)

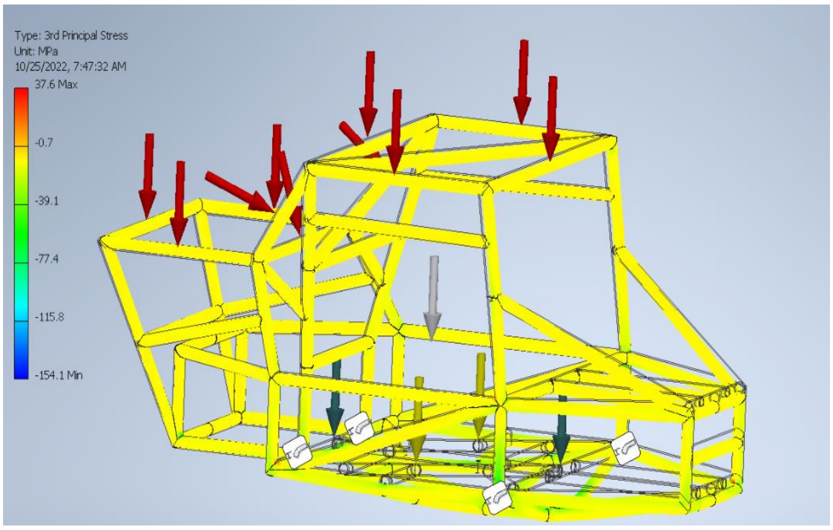

(c)

Figure 9. The 3rd principle stress variation for (a) Design 1, (b) Design 2, and (c) Design 3

Figure 10 shows an increasing trend in terms of 3rd principle stress from design 1 to design 3. The minimum value recorded was -101.1 MPa, -146.9 MPa, and -154.1 MPa for design 1, design 2, and design 3, respectively. Since the third principal stress acts perpendicular to a plane, the value shows that the stress acting as an expansive stress for Design 1 and Design 2. The third principal stress increases as members are removed from the truss structure. This was found similar with Gautam et al. (Gautam et al., 2020). However, removal of truss members further in Design 3 decreasing the third principal stress. This is consistent with the von Misses stress which decreases from Design 2 to Design 3, as shown in **Figure 6**.

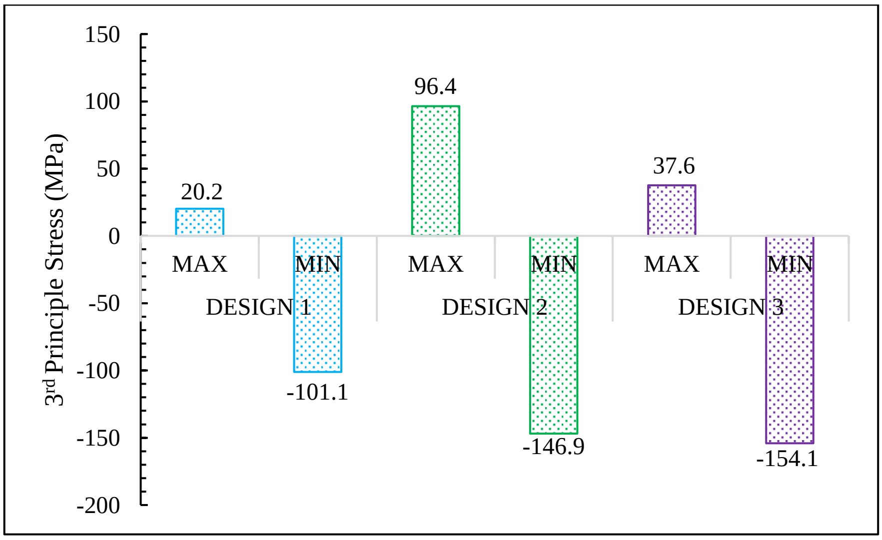

Figure 10. Distribution of 3rd principal stress for the three chassis designs

4. Limitation and Recommendation

Analysis using Autodesk Inventor 2023 limited to static simulation analysis only. Dynamic simulation should be done to better understand the structural integrity for all chassis design. The crash analysis can be done using dynamic simulation from front side, rear side, and side impact. This can be done using advanced Finite Element Analysis (FEA) analysis software such as Ansys. Furthermore, the future tests should be done both in static and dynamic simulation with different materials and in physical form. This may show changes in results and a better material may be found for the chassis.

5. Conclusion

The static analysis of the roll cage chassis by removing truss members from each of the designs shows a variation of static analysis performance. Generally, Design 3 shows an improvement in results in terms of static analysis performance compared to other designs. This is due to fewer members being present in Design 3 which reduces the weight and dependent force of members on each other significantly. The lowest safety factor from design 1, design 2 to design 3 is 2.13, 1.85 to 3.24, respectively. The highest 1st principal stress is 97.39 MPa, 329.5 MPa, and 104 MPa for design 1, design 2, and design 3, respectively. This result is good as the ultimate strength of high carbon steel is 695 MPa. The highest 3rd principal stress is 20.2 MPa, 96.4 MPa, and 37.6 MPa for design 1, design 2, and design 3, respectively. Removing the truss members from the bottom part of the chassis thus give a significant impact on the static analysis of each of the chassis designs. However, fewer truss members do not reflect the overall performance of the structural integrity of the chassis. This is due to the non-conventional design of the chassis itself.

Acknowledgement

The authors would like to thank SEGi University for supporting the research of this study.

References

Abbas, A. H. & Mohammed, A. W. A. (2015). *Dune Buggy Design*.

Buonamici, F., Carfagni, M., Furferi, R., Volpe, Y., & Governi, L. (2020). Generative design: An explorative study. *Computer-Aided Design and Applications, 18*(1), pp. 144–155.

Chauhan, A., Naagar, L., & Chawla, S. (2016). Design and analysis of a Go-kart. *International Journal of Aerospace and Mechanical Engineering*, 3(5), pp. 29-37.

Dimitrijevic, N. J., & Dimitrijevic, B. B. (2020). Generating of technical drawing and associative functionality in Autodesk Inventor. *Knowledge-International Journal*, 43(3), pp. 557-562.

Garg, S., & Raman, R. S. (2013). Design analysis of the roll cage for all-terrain vehicle. *International Journal of Research in Engineering and Technology*, 2(9), pp. 333-338.

Gautam, G. D., Singh, K. P., Prajapati, A., & Norkey, G. (2020). Design optimization of roll cage for formula one vehicle by using finite element analysis. *Materials Today: Proceedings*, 28, pp. 2068–2076.

Krishnamoorthi, S., Prabhu, L., Shadan, M. D., Raj, H., & Akram, N. (2021). Design and analysis of electric Go-Kart. *Materials Today: Proceedings*, 45, pp. 5997–6005.

Lai, H. F., & Xiao, W. Z. (2012). The analysis on the typical parts in F1 race car. *Applied Mechanics and Materials*, 215, pp. 1136–1139.

Li, S., & Feng, X. (2020). Study of structural optimization design on a certain vehicle body-in-white based on static performance and modal analysis. *Mechanical Systems and Signal Processing*, 135, pp. 106405.

Menacho-Mendoza, E., Cedamanos-Cuenca, R., & Díaz-Suyo, A. (2022). Stress analysis and factor of safety in three dental implant systems by finite element analysis. *The Saudi Dental Journal*, 34(7), pp. 579–584.

Mishra, S. (2017). Static analysis of the roll cage of an all-terrain vehicle (SAE BAJA). *International Research Journal of Engineering and Technology*, 4(9).

Munford, P., & Normand, P. (2015). Mastering Autodesk Inventor 2016 and Autodesk Inventor LT 2016: Autodesk Official Press. John Wiley & Sons.

Prakhar, A., Nitish, M., & Shubham, K. (2017). Design, simulation, and optimization, of multitubular rollcage of an all-terrain vehicle. *International Research Journal of Engineering and Technology*, 4(10), pp. 813-820.

Reiter, M., Wehr, M., Sehr, F., Trzuskowsky, A., Taborsky, R., & Abel, D. (2017). The IRT-buggy–vehicle platform for research and education. *IFAC-PapersOnLine*, 50(1), pp. 12588–12595.

Safiuddeen, T., Balaji, P., Dinesh, S., ShabeerHussain, B. M., & Giridharan, M. R. (2021). Comparative design and analysis of roll cage for automobiles. *Materials Today: Proceedings*, 39, pp. 183–200.

Soundararajan, R., Ajith, R., Kumar, C. M., Sabarivasan, U., & Mourya, J. S. (2021). A novel approach for design and analysis of an all-terrain vehicle roll cage. *Materials Today: Proceedings*, 45, pp. 2239–2247.